Source: ASME JCISE-21-1403

Title: FUNCTIONAL REQUIREMENTS OF SOFTWARE TOOLS FOR LASER-BASED POWDER BED FUSION ADDITIVE MANUFACTURING FOR METALS

Authors:

Shaw C. Feng[1]
Systems Integration Division
Engineering Laboratory
National Institute of Standards and Technology
100 Bureau Drive, MS 8260
Gaithersburg, MD 20899
shaw.feng@nist.gov

Tesfaye Moges
Indian Institute of Technology Delhi, New Delhi, India
Tesfaye_mom@yahoo.com

Hyunseop Park
Pohang University of Science and Technology, Pohang, South Korea
hyunseop.park@postech.ac.kr

Mostafa Yakout
McMaster University, Hamilton, Ontario L8S 4L7, Canada
mohamemy@mcmaster.ca

Albert T. Jones
Systems Integration Division
Engineering Laboratory
National Institute of Standards and Technology
100 Bureau Drive, MS 8260
Gaithersburg, MD 20899
albert.jones@nist.gov

Hyunwoong Ko
School of Manufacturing Systems and Networks, Arizona State University, Mesa, AZ 85212, USA
hyunwoong.ko@asu.edu

Paul Witherell
Systems Integration Division
Engineering Laboratory
National Institute of Standards and Technology

[1] Corresponding author: shaw.feng@nist.gov

100 Bureau Drive, MS 8260
Gaithersburg, MD 20899
paul.witherell@nist.gov

ABSTRACT

Additive manufacturing (AM) for metals is rapidly transitioning to an accepted production technology, which has led to increasing demands for data analysis and software tools. The performance of Laser-Based Powder Bed Fusion of Metals (PBF-LB/M), a common metal AM process, depends on the accuracy of data analysis. Advances in data acquisition and analysis are being propelled by an increase in new types of in-situ sensors and ex-situ measurement devices. Measurements taken with these sensors and devices rapidly increasing the volume, variety, and value of PBF-LB/M data but decreasing the veracity of that data simultaneously. The number of new, data-driven software tools capable of analyzing, modeling, simulating, integrating, and managing that data is also increasing; however, the capabilities and accessibility of these tools vary greatly. Issues associated with these software tools are impacting the ability to manage and control PBF-LB/M processes and qualify the resulting parts. This paper investigates and summarizes the available software tools and their capabilities. Findings are then used to help derive a set of functional requirements for tools that are mapped to PBF-LB/M lifecycle activities. The activities include product design, design analysis, process planning, process monitoring, process modeling, process simulation, and production management. PBF-LB/M users can benefit from tools implementing these functional requirements implemented by (1) shortening the lead time of developing these capabilities, (2) adopting emerging, state-of-the-art, PBF-LB/M data and data analytics methods, and (3) enhancing the previously mentioned AM-product-lifecycle activities.

Keywords: additive manufacturing software, data analytics, functional requirements, product lifecycle engineering.

1. INTRODUCTION

The case [1] has been evident that Additive Manufacturing (AM) processes need integrated suites of data analytics (DA) software tools, physics-based models [2], and simulation tools [3]. Continuous development in sensor and monitoring technologies have only heightened these needs. Needed capabilities of software tools [1] have previously been identified to include (1) defect characterization, identification, and rectification [4, 5, 6], (2) physics-based simulation models [7], (3) establishment of relationships between microstructure evolving and temperature change [8], (4) prediction of mechanical properties [9], and (5) validation of parts [10]. As a note, these needs have a focus on the Laser-Based Powder Bed Fusion for Metals (PBF-LB/M) process [11]. For instance, there is a software tool that uses sensor data and models to make predictions about the stabilities and variations in PBF-LB/M processes. Addressing these needs [12] is necessary for AM companies to ensure that they can fulfill quality requirements [13].

A 2018 roadmap by America Makes [14] addressed issues related to combining various DA models, physics-based models, and simulation models. The roadmap noted that the technical and integration gaps associated with combining such models must be addressed. These gaps include (1) building and integrating different types of modeling tools [15, 16, 17], (2) modeling and simulating powder bed fusion processes [18], and (3) accurately estimating part properties [19].

In focusing on metals AM, many efforts are related to the PBF-LB/M. In Section 2, we review the current capabilities of related software tools with three main goals. The first goal is to understand the currently available software tools for critical lifecycle applications. The second goal is to use the results of the first goal to propose a new set of functional requirements for software tools to advance AM functions in industrial applications. The third goal is to use the results of the previous goals to identify high-level gaps and challenges associated with using these software tools in AM systems. Based on [20, 21, 22, 23], we also provide an overview of the required capabilities that these tools should have for PBF-LB/M AM applications. In this paper, we focus on applications that include AM part design, powder spreading, laser melting [24], part solidification [25], grain growth [26], phase transition [27], mechanical property estimation, and residual stress calculations [28].

Section 3 identifies a set of functional requirements for AM data-driven analytic tools for improving the quality of PBF-LB/M AM parts. Section 4 concludes the outcomes of the paper and future work.

2. REVIEW OF PBF-LB/M SOFTWARE TYPES AND FUNCTIONS

There is a variety of available software tools that can assess the state and the quality of fabricated parts at various stages of the PBF-LB/M AM lifecycle. A review of these tools can be found [28]. Using these tools to analyze AM data can lead to new insights into the complexity of AM and knowledge that can enhance quality, increase productivity, and reduce costs. For example, recent advances in Artificial Intelligence (AI) tools, such as machine learning (ML), can make predictions, optimize performance, and detect defects [29]. Currently, several software tools from the research community are available for defect detection in PBF-LB/M using in-situ images coupled with ex-situ X-ray Computed Tomography (XCT) scan models [30]. The underlying techniques implemented in these tools include classification, regression, and forecasting. ML and DA algorithms, including design, process plan, build, post processing, and testing and validation, have been used in AM [13].

2.1 Design modeling and analysis

In design, there are two major activities: modeling and analyzing. The output of the first activity is a design model that includes a representation of part's geometry, features, surface roughness, datum references, lattice structures, and geometric dimensioning and tolerancing (GD&T). Design modeling can also include the use of topology optimization (TO) techniques to determine the optimum topology of the part based on minimizing various mechanical criteria (e.g., weight) and objecting an optimum distribution of material inside a predefined design domain for a given set of loads and boundary conditions [31]. The typical TO objective function is to minimize part compliance while constraining the design space to a predefined volume fraction [32]. The integration of TO into design modeling for the PBF-LB/M can be very effective in designing and producing intricate, lightweight structures. Other build considerations should be addressed when performing TO, such as minimum build angle, minimum feature size, bores, gaps, wall thickness, and overhangs [31]. The second step in design is analyzing the design models. Analyzing these models provides information that allows users to decide whether the proposed design will meet the required specifications. This information is used to create a polygonal mesh that consists of vertices, edges, and faces. This mesh is represented in the STereoLithography (STL) file format, which is an input to the PBF-LB/M controller. An STL file can be developed directly using a polygon-based 3D modeling software or can be generated from Computer-Aided Design (CAD) models using most CAD software systems. Polygonal models can have issues, such as degenerated triangles, self-intersections, internal gaps, and cracks [33].

2.2 Material selection

Material selection plays a key role in the PBF-LB/M process. For instance, the selection of powder feedstock has many factors, such as powder size distribution, morphology distribution, physical properties, and chemical composition. Cost consideration is out of the scope of this study. There are several material databases available for choosing powder materials for the PBF-LB/M process. Many software systems are also available to provide searching and recommendation for the material.

2.3 Process planning, analysis, and monitoring

In process, there are three major PBF-LB/M activities: planning, analyzing, and monitoring. Process planning involves (1) setting up the machine, workpiece on the build platform, and feedstock, (2) determining the support-structure locations, (3) slicing the design into layers, and (4) defining the scan strategy, including process parameters and other control-related settings. Process parameters will affect the quality of parts produced. Control-related parameters may include the heat source parameters, layer thickness, substrate conditions, and powder feeding mechanism [34].

In process analysis, modeling, and simulation, a variety of physics-based simulation models are used to better understand the layer-by-layer processing and the results. Typical models include powder spreading, laser-powder interactions, melt-pool formation, melt-pool solidification, grain growth, phase transition, property modeling, and residual stress estimation [35].

In process monitoring, a variety of remote sensors collect different types of data. PBF-LB/M sensors include high-speed cameras [36, 37], thermal cameras [38 , 39], and acoustic emission sensors [40]. The data collected from these sensors can help determining the current state of the layer-by-layer fabrication process. The images from sensors are used to identify the current state of melting, cooling, pluming, spattering, track formation, and solidification. The output of these models can be used to track the transformation from powder to part. There are models that represent the melting and solidification stages such as balling phenomenon, pore formation, spattering, vaporization of alloying elements, etc. [41].

2.4 Part properties

In property, the key activity is to test and report the mechanical properties of the fabricated part. Mechanical properties are closely related to microstructure and post-processes. The microstructural analysis activity involves estimating the part's microstructure based on images from scanning electron microscope (SEM), including electron back-scattered diffraction (EBSD) SEM. Post-processing activities involve heat treatment, porosity reduction, machining, polishing, and part inspection. Post-process observations are based on dimensional, surface, and volumetric measurements such as those from XCT scanning machines, surface-roughness measuring instruments, and coordinate measuring machines (CMM). The results of these various activities can be integrated into a framework for investigating the process-structure-property (PSP) relationships in PBF-LB/M AM. For example, the thermal and mechanical properties of AM parts can be tailored by controlling the process parameters [42]. These properties include tensile, fatigue, compressive, creep, thermal expansion, and conductivity. Therefore,

it is necessary to model the PSP data to find the relationship between input process parameters and output part properties.

2.5 Product lifecycle management

Section 2.3 discusses the functions required for selecting the feedstock material. In this section, material management, product lifecycle management, and part validation are discussed. Material management is a function of managing material data for material selection, traceability on part performance, and process validation. Product lifecycle management is a function of managing the product data for optimizing design, planning, quality, and delivery. Part validation may include contributions from the previously identified stages as well as additional requirements. Generally, it is a process of validating the material, equipment, and production process for the quality of the PBF-LB/M parts.

2.6 Software Capabilities

The above-mentioned activities can collect data from several types of in-situ and ex-situ measuring equipment. In-situ sensors have been used for PBF-LB/M process monitoring by researchers and manufacturers. Ex-situ inspection instruments include photogrammetry, scanning instruments, pyrometers, XCT instruments, and CMMs. In-situ sensors collect data in two different setups: coaxial with the laser axis and off-axis (staring). The data from these measuring instruments can be used collectively to determine the state of the PBF-LB/M process and predict any defects in workpieces [43]. To do so, however, the data must be traced back to the process state and integrated into a suite of datasets for DA and decision-making. It is important to understand functional requirements, analytic methods, and commonly used PBF/LB-M AM systems [44]. We use this decomposition of capabilities to guide the derivation of the desired functional requirements for AM data management in Section 3.

3. FUNCTIONAL REQUIREMENTS OF PBF-LB/M SOFTWARE TOOLS

This section presents a set of functional requirements (see [45]) associated with the five aspects described above. Figure 1 shows the workflow of the functional requirements. In this section, those

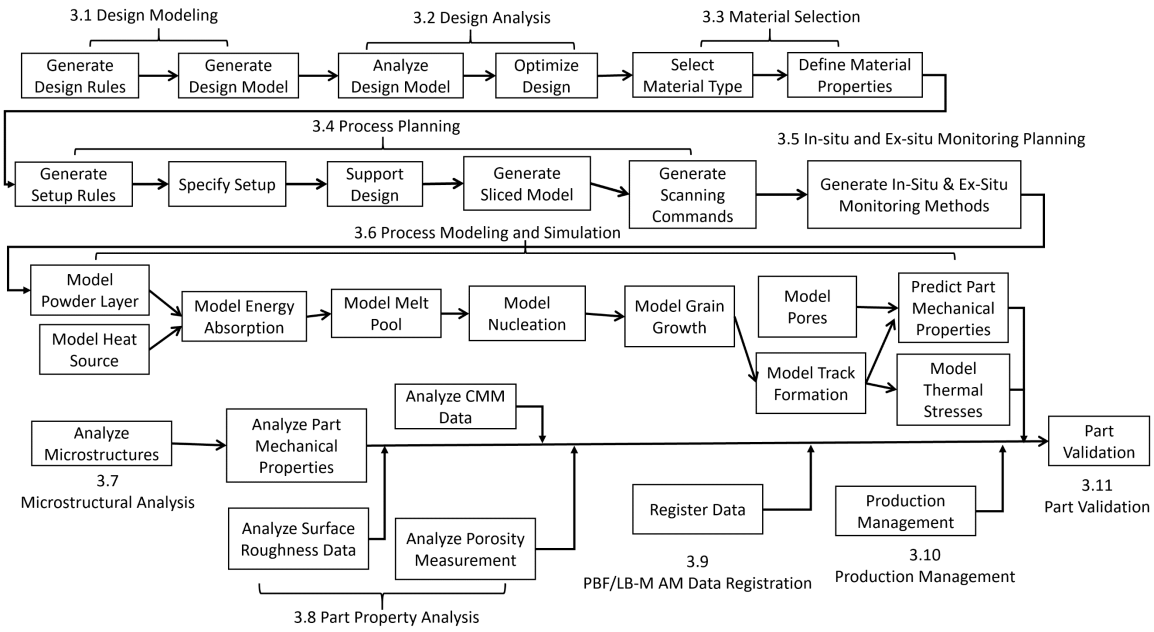

Figure 1 Functional requirement architecture - workflow

requirements are not formulated mathematically, just linguistically. Each function relates its input data to output data; the format is (Output_Data) = Function (Input_Data).

3.1 Design Modeling

In AM, design-modeling functions are used to design parts. AM refers to the ability of materials to be joined layer-upon-layer together successfully (e.g., without manufacturing failures or defects such as undesired warping and internal cracks due to material properties or process parameters) [46]. The functional requirements are described in the following two functions.

Design_Rules = GenerateDesignRules(AM_Feature, Material_Properties, AM_Machine_Capabilities, Geometry) (1)

This function generates Design_Rules that guide designers to create the geometries, structures, tolerances, datums, and surface roughness constraints for an AM part. The AM_Feature input includes 1) any information or knowledge about manufacturable features using AM [47] and 2) design intents and AM context, which are reflected in 2D or 3D models in both geometric surface and volume [48]. These features include overhang features, support structures, self-supporting structures, and thin wall features [49, 50]. The Material_Properties input includes information about material composition, physical properties, powder shapes, powder flowability, and size distributions. The AM_Machine_Capabilites input includes maximum power, work volume, maximum speed, inert gas, feedstock feeding mechanism, build platform, and the range of layer thickness. The Geometry input includes geometric representations constrained by both the AM machine capabilities and the material properties. The information associated with those properties include wall thickness, overhang length,

and undercut angle, among others. The output of this function is a set of Design_Rules that guide designers or software tools to design 3D models of AM parts. Design rules specify the range of allowable deviations of an AM_Feature, given machine and material constraints. Some examples of design allowable include shapes, size, orientations, and support structure with their allowable variations. The range constraints specify the magnitude of those deviations, and the inputs provide those constraints. Design_Rules specify design guidelines for the design allowable in specified rule formats.

Design_Model = GenerateDesignModel(Design_Rules, Design_Requirements) (2)

This function uses the designated Design_Rules to create a geometric model that includes those design allowable. The inputs to this function are the Design_Rules and Design_Requirements that include the maximum porosity, tensile strength, fatigue life, tolerances, and surface roughness. The output is a Design_Model, which can be either an enhanced 3D tessellated model or a solid-geometric model.

3.2 Design Analysis

Design analysis helps the manufacturer create a Design_Model by producing a Design_Analysis_Report [51]. This report is the output of the following functions.

Design_Analysis_Report = AnalyzeDesignModel(Design_Model, Design_Requirements) (3)

This function analyzes the current Design_Model based the Design_Requirements [52]. These include mechanical strength, fatigue life, geometric tolerances, and surface roughness. The output is the Design_Analysis_Report, which estimates the product performance and design parameters.

Optimized_Model = OptimizeDesign(Objective_Function, Design_Rules, Design_Analysis_Report, Design_Model, Design_Requirements) (4)

This function optimizes a part design given the Objective_Function, Design_Rules, Design_Model, Design_Analysis_Report, and the Design_Reqruiements [53]. Objective_Function is used for optimization. For example, maximize product performance. Doing so would involve three types of Design_Model analyses: structural, tolerance, and fluid-flow. A structural analysis ensures that the designed part can meet the expected loads when the part is in use. A tolerance analysis ensures that the AM part is within the specified tolerances [54, 55]. A fluid-flow analysis ensures that the designed part meets all requirements of fluid mechanics. The output is an Optimized_Model, either a 3D tessellated or solid-geometric model that includes the lattice or the topological structure. Design_Rules are used to ensure that the final structure must maintain a certain level of manufacturability considering given constraints without compromising the part's Design_Requirements [48]. Various, topology-optimization techniques can be used to modify the part design based on the functional requirements and the material-distribution specifications associated with the volume of the structure [56, 57]. It is necessary to optimize the design for weight reduction, load distribution, thin walls, and internal features. The results will enhance part functionality and avoid producing unnecessary features [49].

3.3 Material Selection

Material-selection functions are as follows.

Material_Type = SelectMaterialType(Design_Rules, Design_Model, Design_Requirements, Material_Property_Data, Material_Availability_Data) (5)

This function selects a specific material type based on the design model, design rules, design requirements [58], material property data, and material availability data. Material types include stainless steel, titanium alloy, or nickel alloy.

Powder_Parameters = DefineMaterialProperties(Material_Type, Design_Model, Mechanical_Property_Requirements) (6)

This function selects the powder parameters based on the selected material type, the current design model, and mechanical property requirements on powder materials. These requirements include powder-size distribution, shape distribution, thermal properties, chemical composition, physical properties, and mechanical properties [41].

3.4 Process Planning

The PBF-LB/M process planning determines how to manufacture a part based on 1) the physical operations of the PBF-LB/M process and 2) the results of all the previous functions. Process planning determines the following functions: Setup_Rules, Setup_Model, Support_Model, Sliced_Model, and Scanning_Commands, which are desired locations and speeds that laser beam has to follow for scanning the part [59, 60]. An example is a part program in G code.

Setup_Rules = GenerateSetupRules(Design_Model, Material_Type, Powder_Parameters, Process_Capability) (7)

This function generates setup rules based on four inputs: Design_Model, Material_Type, Powder_Parameters, and Process_Capability. The latter input includes the maximum laser power, minimum laser spot size, maximum scanning speed, and build platform size. The output is a set of Setup_Rules that can be used to specify how an AM part should be oriented on the build platform [61].

Setup_Model = SpecifySetup(Design_Model, Setup_Rules, Design_Requirements) (8)

This function uses the Design_Model, Setup_Rules, and Design_Requirements to create a Setup_Model that indicates the location and orientation of the part on the build platform [62].

Support_Model = SupportDesign(Setup_Model, Design_Model) (9)

This function designs the support structure for overhangs using Setup_Model and Design_Model as the input parameters. The output parameter is the Support_Model that includes the design geometry as well as any necessary structures to support overhangs [49].

Sliced_Model = GenerateSlicedModel(Support_Model, Machine_Capabilities) (10)

This function generates the Sliced_Model based on the Support_Model and Machine_Capabilities. The output is a Sliced_Model that includes the slices needed to fabricate the various layers of the part.

Scanning_Commands = GenerateScanningCommands (Sliced_Model, Scanning_Strategy, Scanning_Parameters) (11)

This function generates Scanning_Commands for the galvanometer(s), based on the Sliced_Model, Scanning_Strategy, and Scanning_Parameters. The output is a set of Scanning_Commands needed to scan powders layer by layer for building a part [63].

3.5 In-situ and Ex-situ Monitoring Planning

This function prepares the activities needed to monitor PBF-LB/M processes and measure part parameters [64]. The in-situ and ex-situ monitoring planning function is as follows.

Monitoring_Methods = GenerateInSituExSituMonitoringMethods (Design_Model, Scanning_Commands, Sensor_Capabilities, Machine_Capability) (12)

The function generates in-situ and ex-situ monitoring methods by knowing the Design_Model, Scanning_Commands Sensor_Capabilities, and Machine_Capability [65, 66]. The Sensor_Capabilities input defines the characteristics of each sensor including its resolution, measurement ranges, sampling speed, sensitivity, and magnification. The output is a set of Monitoring_Methods to monitor the melting and solidification of the AM part during PBF-LB/M.

3.6 Process Modeling and Simulation

Physics-based modeling methods and simulation software tools are used to model the physical phenomena associated with PBF-LB/M processes. Physics-based models include powder deposition, heat source, melt pool, nucleation, track formation, stress formation, pore formation, and part properties [67].

Powder_Deposition_Model = ModelPowderLayer(Powder_Parameters, Powder_Properties, Powder_Spreading_Mechanism_Parameters, Layer_Properties) (13)

This function builds models of the powder-layer formation during powder spreading, which uses a blade or a roller spreading mechanism while considering the contact forces among the powder particles [68]. Input parameters include sets of Powder_Parameters (e.g., powder shape, size, and distribution), Powder_Properties, and Powder_Spreading_Mechanism_Parameters (e.g., recoater shape, friction coefficient with the powder, and speed) [69]. Layer_Properties include the layer dimensions including the depth, width, and length of a powder layer and defects including streaks, void, and waviness. The output is a physics-based Powder_Deposition_Model that can be used to predict the packing density [70].

Heat_Source_Model = ModelHeatSource(Laser_Parameters)

This function builds a heat-source model, which is used to estimate the amount and distribution of the heat emitted from a laser beam onto the powder layer with Laser_Parameters as input [71]. Laser_Parameters include the laser power, spot size, and powder distribution. This heat source model describes the amount of deposited energy per unit time and affects melt pool characteristics such as melt pool dimensions and temperature gradients.

Energy_Absorption_Model = ModelEnergyAbsorption(Heat_Source_Model, Powder_Deposition_Model, Material_Properties, Scanning_Commands, Inert_Gas_Parameters) (14)

This function builds an Energy_Absorption_Model to analyze the amount of energy absorbed by the powders in each layer. This function uses the Heat_Source_Model, Powder_Deposition_Model, and Material_Properties as inputs [72, 73]. Material_Properties are the absorption coefficient for absorptivity and thermal conductivity of the powders. Creating this function needs physics-based knowledge about the heat absorptivity, reflectivity, metal liquid flow, plume formation, spattering,

evaporation, and cooling. This Energy_Absorption_Model is needed for building a melt pool model, which is needed for estimating the nucleation, grain growth, thermal stress, and pore formation. Scanning_Commands include scan speed, laser power, and spot size. Inert_Gas_Parameters define the type and the nominal flow rate of the inert gas in the build chamber that affects melt pool geometry and porosity [74].

Melt_Pool_Model = ModelMeltPool(Energy_Absorption_Model, Powder_Deposition_Model, Heat_Source_Model, Material_Properties, Scanning_Commands, Inert_Gas_Parameters) (15)

This function identifies models for powder melting, heat transfer, and fluid flow in a melt pool [75]. Input parameters include sets of Powder_Deposition_Model, Heat_Source_Model, Material_Properties, Scanning_Commands, and Inert_Gas_Parameters. The output is a physics-based Melt_Pool_Model that can be imported into a simulation tool to predict the melt-pool evolution [76]. The evolution is based on the models of conduction, convection, evaporation, denudation, keyholing, recoiling, pluming, and spattering [77]. Creating this function needs physics-based knowledge about the liquid flow and heat transfer in the melt-pool evolution. Additionally, the knowledge on pluming, spattering, cooling, and solidification, as mentioned above is also needed for creating this function. Melt_Pool_Model is used to simulate liquid metal behaviors during laser scanning.

Nucleation_Model = ModelNucleation(Melt_Pool_Model, Material_Chemical_Composition, Material_Properties_Grain_Growth, Cooling_Rate) (16)

This function generates a model of nucleation that describes the density changes of the nucleus as the metal liquid transforms into a solid [78]. The model includes nucleus density vs. temperature, phases of nuclei, the grain orientation of each nucleus, the size of each nucleus, and the atomic structure of a nucleus. The model is needed for modeling grain growth. Input parameters are as follows. Melt_Pool_Model is described above. Material_Chemical_Composition includes percentages of all the chemical components in the powders. Material_Properties_Grain_Growth is a set of parameters [79] that includes thermal gradients that are calculated from the melt pool model, the undercooling temperature of liquid metal, the surface tension of the metal liquid, viscosity, solidus temperature, liquidus temperature, latent heat, diffusion coefficients of alloy elements in both liquid and solid, grain boundary mobility, liquid and solid densities, specific heat, and Gibbs-Thompson coefficient. Cooling_Rate is derived from scanning speed, which is from the laser beam control commands consisting of a sequence of laser spot locations at specific times, scanning speed, thermal properties in Material_Properties, and Melt_Pool_Model. A nucleation model is essential for modeling grain growth in a forming track.

Track_Formation_Model = ModelTrackFormation (Nucleation_Model, Material_Properties_Grain_Growth) (17)

This function provides a model of the laser-scanned track formation during cooling and solidification [80]. The model is based on the a grain growth model that 1) describes phase changes from liquid to solid, 2) the grain boundary changes as the temperature decreases during solidification and as it increases based on surface and bulk energy, and 3) the phase change in the solid [81]. The grain growth results in a track of solid metal in the scan path. A slightly different grain growth can come from keyholing [82], which should be included. The input parameters are Nucleation_Model and Material_Properties_Grain_Growth. The output is a Track_Formation_Model, which describes sizes,

phases, and orientations of grains that form the track. A Track_Formation model is essential for modeling thermal stress in the part.

Stress_Formation_Model = ModelThermalStresses (Track_Formation_Model, Thermal_Characteristics, Mechanical_Properties) (18)

This function generates a model of thermal stresses based on the Track_Formation_Model, the Thermal_Characteristics, and the Mechanical_Properties. Thermal_Characteristics include thermal history (time) and temperature profile (location) in the workpiece. Mechanical_Properties are those thermo-mechanical properties, including plastic tangent modulus, Young's modulus, yield strength, thermal expansion coefficient, Poisson's ratio, thermal diffusivity, thermal conductivity, and specific heat capacity. These properties are needed to calculate the thermal stresses distribution in the fabricated part [83]. The distribution is essential for modeling and predicting part mechanical properties.

Pore_Formation_Model = ModelPores(Powder_Deposition_Model, Heat_Source_Model) (19)

This function generates a model that is used to investigate the internal pore formation in the part during scanning in the chamber with inert gas. Internal pores can come from tiny gas bubbles in the powder, gas entrapped during melt flow [84], and keyholing [82]. The inputs include Powder_Deposition_Model and Heat_Source_Model. These inputs determine the liquid metal flow in the melt pool and pore entrapment in the liquid and during solidification. Given the powder-material properties and the heat source, we assume that pore formation depends mostly on the fluid characteristics in the melt pool. These fluid characteristics are determined primarily by the thermal characteristics, which include the maximum temperature, heat gradient, and cooling rates, thermal history, and temperature profile [85]. A Pore_Formation_Model is essential for modeling the part's mechanical properties.

Part_Mechanical_Properties = PredictPartMechanicalProperties(Track_Formation_Model, Pore_Formation_Model, Design_Model) (20)

The function models and predicts mechanical properties of the part [80]. Mechanical properties include material strength, fatigue life, and hardness. The input includes the Grain_Growth_Model, Thermal_Characteristics of solidification, and Design_Model. The Design_Model affects part properties, e.g., anisotropy in the part. The output includes the predicted Part_Mechanical_Properties.

3.7 Microstructural Data Analysis

Microstructural data analysis is needed to report the material properties of additively manufactured parts based on microstructure images. Those images are obtained from a variety of measurement instruments such as EBSD SEM [86].

Microstructure_Characterization = AnalyzeMicrostructures (Image_Sets) (21)

This function characterizes the grain structures (sizes, orientations, and phases) and microstructural defects, including any abnormal residual stress concentrations. The inputs are Image_Sets that include images and three-dimensional models, which are built from a stack of two-dimensional images. Meta data about the microscope and the data acquisition, including cross-sectioning, grinding, polishing, etching, microscopy settings, and microscope capabilities should also be associated with the Image_Sets. The output is a Microstructure_Characterization including grain structures and defects.

3.8 Part Property Analysis

From part property analysis, the mechanical, dimensional, and surface properties of the part are estimated based on data obtained from measurements and mechanical tests. Mechanical properties include tensile strength, torsional strength, fatigue life, and hardness. Dimensional measurements are used to verify whether the fabricated part features meet the tolerance requirements specified in the design. Surface properties are primarily based on surface roughness measurements. Additionally, pore analysis is generated from the porosity measurements.

Part_Mechanical_Property_Characterization = AnalyzePartMechanicalProperties (Microstructure_Characterization, Mechanical_Property_Data) (22)

This function analyzes a post-processed part. Inputs are Microstructure_Characterization and Mechanical_Property_Data. Mechanical_Property_Data is from mechanical property tests, such as tensile strength, torsional strength, fatigue life, and hardness. The output is a Part_Mechanical_Property_Characterization on the measured mechanical properties from the mechanical property tests.

Measured_Feature_Model = AnalyzeCMMData (Point_Cloud) (23)

This function analyzes data collected from coordinate measurements using, e.g., a coordinate measuring machine (CMM). The data is in a point cloud that is used for feature analysis. The output is the Measured_Feature_Model. The Measured_Feature_Model is used to determine if the measured features are within specified dimensional and geometric tolerances.

Surface_Roughness = AnalyzeSurfaceRoughnessData(Surface_Topography_Data) (24)

This function characterizes surface roughness based on Surface_Topography_Data, which is collected from a surface-roughness-measuring instrument. The output is a set of Surface_Roughness values in R_a or other standardized definitions of all the measured surfaces.

Porosity = AnalyzePorosityMeasurement(Porosity_Data) (25)

This function uses the measured Porosity_Data to analyzes the porosity of an AM fabricated part. Porosity_Data can be generated from nondestructive measurements, such as XCT scanners. The output is the measured Porosity of an AM part.

3.9 PBF/LB-M AM Data Registration

Data registration [87] is a function to catalog measured data for validation.

Registered_Data = RegisterData(Measured_Data, Meta_Data) (26)

This function supports the data registration process that has three major sub-processes. The first is to couple sensor-related data and build-related data with the raw measured data. The second transforms the coupled data related from each local coordinate systems to a single, common, coordinate system. The third assigns an identifier (ID) to the data for future reference and validation. The inputs to this function include Measured_Data and its associated Meta_Data, which is the type of data that provide the context of the data, such as the sensor parameters, sensor configurations, sensor setup, data

format, build data, and uncertainty in measurement [88]. The output is used in downstream applications.

4. CONCLUSIONS AND FUTURE WORK

The demands on new software tools for PBF-LB/M AM have increased because the volume, variety, and importance of data have rapidly increased. However, a data's value is based on its veracity, which is still cannot be measured accurately. Simultaneously, its veracity is critical because data are used as the inputs to software tools that currently implement several lifecycle functions in industrial applications. These functions include design, material selection, process-parameter setting, microstructural analysis, and part-property prediction. Currently, however, more software tools are needed for defect detection, root cause analysis, and predicting the quality of fabricated parts are needed. For example, sensor data analytics algorithms for image analysis from in-situ and ex-situ measurements to detect pores and cracks shown in the XCT images. The pores must be correlated to lack-of-fusion or keyholing using the melt pool thermal data or melt depth measurements from X-ray imaging.

This paper identifies specific data types and functional requirements for using DA tools to enhance PBF/LB-M AM product lifecycle functions. Those functional requirements relate output data to input data, based on physical principles. The identified data types and functional requirements will help AM technology users address challenges related to (1) adopting emerging, state-of-the-art, AM data and DA methods and (2) the use of sensor data to enhance AM product lifecycle activities, such as design, process control, and part qualification. In addition, some commonly used algorithms for DA are mentioned in this paper. These algorithms are developed for general machine learning and statistical analysis tools, and more specific algorithms for AM systems are needed. Integrating the material, process, property, and performance relationships into these new AM algorithms is required.

For future work, we will explore and address new functions that are not used in any current commercial software tools for AM. We will also address how to manage the identified, very complex input-output data objects. The AM-specific data objects include material property parameters, pores, scanning strategies, tessellation, grain structures, and post-process measurements. For handling these data that is becoming big and complex, we intend to develop an architecture that will facilitate querying, reusing, and sharing that data in cyber-physical systems. Lastly, some commonly used algorithms for DA are mentioned in this paper. These algorithms were developed for general ML and statistical analysis. More specific algorithms for AM problems will be needed. Finally, determining the correlations among material, process, property, and performance will be needed before AM manufacturers can use these new, specific AM algorithms.

DISCLAIMER

REFERENCES

[1] Measurement Science Roadmap for Metal-Based Additive Manufacturing, the National Institute of Standards and Technology, May 2013.

[2] Moges, T., Yang, Z., Jones, K., Feng, S., Witherell, P., and Lu, Y. (2020) "Hybrid modeling approach for melt pool prediction in laser powder bed fusion additive manufacturing," *J. Computing and Information Science in Engineering*, Vol. 21, No. 5, Oct 2021, paper #: JCISE-20-1259.

[3] Yan, W., Lin, S., Kafka, O., Lian, Y., Yu, C., Liu, Z., Yan, J., Wolff, S., Wu, H., Ndlp-Agbor, E., Mozaffar, M., Ehmann, K., Cao, J., Wagner, G., and Liu, W., "Data-driven multi-scale multi-physics models to derive process–structure–property relationships for additive manufacturing," Computational Mechanics, Vol. 61, 2018, pp. 521–541.

[4] Di Angelo, L., Di Stefano, P., and Guardini, E., "Search for the Optimal Build Direction in Additive Manufacturing Technologies: A Review," J. Manufacturing and Materials Processing, Vol. 4, No. 71, 2020.

[5] Ye, D., Fuh, J., Zhang, Y., Hong, G., and Zhu, K., "In situ monitoring of selective laser melting using plume and spatter signatures by deep networks," ISA Transactions, Vol. 81, 2018, pp. 96 – 104.

[6] Ye, D., Hong, G., Zhang, Y., Zhu, K., Fuh, J., "Defect detection in selective laser melting technology by acoustic signals with deep belief networks," International Journal of Advanced Manufacturing Technology, 2018, pp. 1–11.

[7] Yan, W., Lin, S., Kafka, O., Lian, Y., Yu, C., Liu, Z., Yan, J., Wolff, S., Wu, H., Ndlp-Agbor, E., Mozaffar, M., Ehmann, K., Cao, J., Wagner, G., and Liu, W., "Data-driven multi-scale multi-physics models to derive process–structure–property relationships for additive manufacturing," Computational Mechanics, Vol. 61, 2018, pp. 521–541.

[8] Chadwick, "The Development of Grain Structure During Additive Manufacturing," Acta Materialia, Vol. 211, 2021, #116852.

[9] Baulfeld, B., Van der Biest, O., and Gault, R., "Additive Manufacturing of Ti-6Al-4V Components by Shaped Metal Deposition: Microstructure and Mechanical Properties," J. Materials and Design, Vol. 31, 2010, S106-S111.

[10] Grasso, M. and Colosimo, B., "Process defects and in situ monitoring methods in metal powder bed fusion: a review," Journal of Measurement Science and Technology, Vol. 28, 2017, doi:10.1088/1361-6501/aa5c4f.

[11] ISO/ASTM 52911-1:2019, Additive manufacturing - Design - Part 1: Laser-based powder bed fusion of metals, International Organisation for Standardization, 2019.

[12] NASA/NIST/FAA Report on Computational Materials Approaches for Qualification by Analysis for Aerospace Applications, NASA/TM-20210015175, May 2021.

[13] Razvi, S., Feng, S., Lee, Y., Witherell, P., Narayanan, A., "A Review of Machine Learning Applications In Additive Manufacturing," Proceedings of the ASME 2019 IDETC/CIE, paper number: 98415, August 2019.

[14] Standardization Roadmap For Additive Manufacturing, Version 2, America Makes, Youngs Town, PA, 2018.

[15] Abdelrahman, M., Reutzel, E., Nassar, A., and Starr, T., "Flaw Detection in Powder Bed Fusion Using Optical Imaging," Journal of Additive Manufacturing, Vol. 15, 2017, pp. 1 – 11.

[16] Bartlett, J., Heima, F., Murty, Y., and Lia,X., "In situ defect detection in selective laser melting via full-field infrared thermography," Journal of Additive Manufacturing, Vol. 24, 2018, pp. 595 – 605.

[17] Cheng, B., Lydon, J., Cooper, K., Cole, V., Northrop, P., and Chou, K., "Melt pool sensing and size analysis in laser powder-bed metal additive manufacturing," Journal of Manufacturing Processes, Vol. 32, 2018, pp. 744- 753.

[18] Mukherjee, T., Wei, H., De, A., and DebRoy, T., "Heat and Fluid Flow in Additive Manufacturing – Part I: Modeling of Powder Bed Fusion," J. Computational Materials Science, Vol. 150, 2018, pp. 304 – 313.

[19] DebRoy, T., Wei, H., Zuback, J., Mukherjee, T., et al., "Additive Manufacturing of Metallic Components – Process, Structure, Properties," Progress in Material Science, Vol. 92, 2018, pp. 112 – 224.

[20] National Academies of Sciences, Engineering, and Medicine, "Data-Driven Modeling for Additive Manufacturing of Metals: Proceedings of a Workshop," Washington, DC: The National Academies Press, 2019, https://doi.org/10.17226/25481.

[21] Witherell, P., "Emerging Datasets and Analytics for Additive Manufacturing," Proceedings of Fraunhofer Direct Digital Manufacturing Conference DDMC 2018, Fraunhofer Verlag, Berlin, Germany, March 14 – 15, 2018, pp. 43 – 48.

[22] ISO/ASTM 52901:2017 Additive manufacturing — General principles — Requirements for purchased AM parts.

[23] ISO / ASTM52910 – 18 Additive manufacturing — Design — Requirements, guidelines and recommendations.

[24] Gu, H., Gong, H., Pal, D., Rafi, K., Starr, T., and Stucker, B., "Influences of Energy Density on Porosity and Microstructure of Selective Laser Melted 17- 4PH Stainless Steel," Proceedings of the Solid Freeform Fabrication Symposium, 2013.

[25] Purtonen, T., Kalliosaari, A., and Salminen, A., "Monitoring and Adaptive Control of Laser Processes," Physics Procedia, Vol. 56, 2014, pp. 1218 – 1231.

[26] Lian, Y., Gan, Z., Yu, C., Kats, D., Liu, W., Wagner, G., "A cellular automaton finite volume method for microstructure evolution during additive manufacturing," Material and Design, Vol. 169, #107672, 2019.

[27] Li, C., Liu, Z., Fang, X., and Guo, Y., "Residual Stress in Metal Additive Manufacturing," 4th CIRP Conference on Surface Integrity, 2018, pp. 348 – 353.

[28] Feng, S., Moges, T., Witherell, P., "FUNCTIONAL REQUIREMENTS OF DATA ANALYTIC TOOLS AND SOFTWARE FOR METAL ADDITIVE MANUFACTURING," Proceedings of the ASME 2020 International Mechanical Engineering Congress and Exposition, Portland, OR, 2020, IMECE2020-24117.

[29] [Wuest] Wuest, T., Weimer, D., Irgens, C., and Thoben, K.-D., 2016, "Machine Learning in Manufacturing: Advantages, Challenges, and Applications," Prod. Manuf. Res., 4(1), pp. 23–45.

[30] [Petrich 2017] Petrich, J., Gobert, C., Phoha, S., Nassar, A, and Reutzel, E., "Machine Learning for Defect Detection for PBFAM Using High Resolution Layerwise Imaging Coupled With Post-Build CT Scans," Proceedings of the 28th Annual International Solid Freeform Fabrication Symposium – An Additive Manufacturing Conference, 2017, pp. 1363 – 1381.

[31] Reddy, S., Maranan, K., Simpson, T., Palmer, T., and Dickman, C., "Application of Topology Optimization and Design for Additive Manufacturing Guidelines on an Automotive Component," ASME 2016 International Design Engineering Technical Conferences and Computers and Information in Engineering Conference, no. 50107, 2016, p. V02AT03A030.

[32] Li, C., Liu, Z., Fang, X., and Guo, Y., "Residual Stress in Metal Additive Manufacturing," 4th CIRP Conference on Surface Integrity, 2018, pp. 348 – 353.
[33] Gao, W. et al., "The status, challenges, and future of additive manufacturing in engineering," Computer-Aided Design, Vol. 69, 2015, pp. 65-89.
[34] Yakout, M., Cadamuro, A., Elbestawi, M.A., and Veldhuis, S.C., "The selection of process parameters in additive manufacturing for aerospace alloys," The International Journal of Advanced Manufacturing Technology, Vol. 92, 2017, pp. 2081-2098.
[35] Taheri, H., Shoaib, M., Koester, L., Bigelow, T., Collins, P., Bond, L., "Powder-based additive manufacturing - a review of types of defects, generation mechanisms, detection, property evaluation and metrology," Additive and Subtractive Materials Manufacturing, 2017, doi.org/10.1504/IJASMM.2017.088204
[36] Zhao, C. et al., "Real-time monitoring of laser powder bed fusion process using high-speed X-ray imaging and diffraction," Scientific Reports, Vol. 7, 2017, article number: 3602.
[37] Wang, D. et al., "Mechanisms and characteristics of spatter generation in SLM processing and its effect on the properties," Materials & Design, Vol. 117, 2017, pp. 121-130.
[38] Yakout, M., Phillips, I., Elbestawi, M.A., and Fang, Q., "In-situ monitoring and detection of spatter agglomeration and delamination during laser-based powder bed fusion of Invar 36," Optics & Laser Technology, Vol. 136, 2021, 106741.
[39] Zheng, L. et al., "Melt pool boundary extraction and its width prediction from infrared images in selective laser melting," Materials & Design, Vol. 183, 2019, 108110.
[40] Mohammadi, M.G., and Elbestawi, M., "Real Time Monitoring in L-PBF Using a Machine Learning Approach," Procedia Manufacturing, Vol. 51, 2020, pp. 725-731.
[41] DebRoy, T., Wei, H., Zuback, J. et al., "Additive manufacturing of metallic components – Process, structure and properties," Progress in Material Science, Vol. 92, 2018, pp. 112 – 224.
[42] Yakout, M., Elbestawi, M.A., and Veldhuis, S.C., "A study of thermal expansion coefficients and microstructure during selective laser melting of Invar 36 and stainless steel 316L," Additive Manufacturing, Vol. 24, 2018, pp. 405-418.
[43] Grasso, M., Colosimo, B., "Process defects and in situ monitoring methods in metal powder bed fusion: a review," Meas Sci Technol, Vol. 28 No. 044005, 2017, doi:10.1088/1361-6501/aa5c4f.
[44] Measurement Science Roadmap for Metal-Based Additive Manufacturing, the National Institute of Standards and Technology, May 2013.
[45] ISO/IEC/IEEE 31320-1:2012, Information technology – Modeling Languages – Part 1: Syntax and Semantics for IDEF0.
[46] Ko, H, Witherell, P., Lu, Y., Kim, S., and Rosen, D., "Machine learning and knowledge graph based design rule construction for additive manufacturing," J. Additive Manufacturing, Vol. 37, 2021, 101620.
[47] Mani, M., Witherell, P., and Jee, H., "Design Rules for Additive Manufacturing: A Categorization," Proceedings of ASME Design Engineering Technical Conference, Paper number: 68446, 2017.
[48] Ko, H., Witherell, P., Lu, Y., Kim, S., and Rosen, D., "Machine learning and knowledge graph based design rule construction for additive manufacturing," Additive Manufacturing, Vol. 37, 2021, #101620.

[49] Plocher, J., & Panesar, A., “Review on design and structural optimisation in additive manufacturing: Towards next-generation lightweight structures,” Materials & Design, Vol. 183, 2019, #108164.
[50] Zhang, K., Cheng, G., and Xu, L., “Topology Optimization Considering Overhang Constraint in Additive Manufacturing,” Computer & Structures, Vol. 212, 2019, pp. 86 – 100.
[51] Kim, S., Rosen, D. W., Witherell, P., and Ko, H. (June 13, 2019). "A Design for Additive Manufacturing Ontology to Support Manufacturability Analysis." ASME. J. Comput. Inf. Sci. Eng. December 2019; 19(4): 041014. https://doi.org/10.1115/1.4043531
[52] Allison, J., Sharpe, C., and Seepersad, C., “Powder bed fusion metrology for additive manufacturing design guidance,” Additive Manufacturing, Vol. 25, 2019, pp. 239 – 251.
[53] Leary, M., Merli, L., Torti, F., Mazur, M., and Brandt, M., “Optimal topology for additive manufacture: A method for enabling additive manufacture of support-free optimal structures,” Materials & Design, Vol. 63, 2014, pp. 678 – 690.
[54] Xia, Y., Mantzaflaris, A., Juttler, B. et al., “Design of Self-supporting Surfaces with Isogeometric analysis,” Computer Methods in Applied Mechanics and Engineering, Vol. 353, 2019, pp. 328 – 347.
[55] McConaha, M., Venugopal, V., and Anand, S., “Design Tool for Topology Optimization of Self Supporting Variable Density Lattice Structures for Additive Manufacturing,” Manufacturing Science and Engineering, Vol. 143, No. 7, 2021, Paper#: MANU-19-1348.
[56] Sigmund, O. an Maute, K., “Topology optimization approaches,” Structural and Multidisciplinary Optimization, Vol. 48, No. 6, 2013, pp. 1031 – 1055.
[57] Liu, J., Gaynor, A.T., Chen, S. et al. Current and future trends in topology optimization for additive manufacturing. Struct Multidisc Optim, Vol. 57, 2018, pp. 2457–2483.
[58] Zaman, U., Rivette, M., Siadat, A., Mousavi, S., “Integrated product-process design: Material and manufacturing process selection for additive manufacturing using multi-criteria decision making,” Robotics and Computer-Integrated Manufacturing, Vol. 51, 2018, pp. 169 – 180.
[59] Pan, T. et al., “General Rules for Pre-Process Planning in Powder Bed Fusion System - A Review,” Proceedings of the 29th Annual International Solid Freeform Fabrication Symposium (2018, Austin, TX), pp. 1161-1173, University of Texas at Austin, Aug 2018.
[60] Yeung, H., Lane, B., Donmez, M., Fox, J., and Neira, J., “Implementation of Advanced Laser Control Strategies for Powder Bed Fusion Systems,” Procedia Manufacturing, Vol. 26, 2018, pp. 871-879.
[61] Marrey, M., Malekipour, E., El-Mounauri, H., Faierson, E., “A Framework for Optimizing Process Parameters in Powder Bed Fusion (PBF) Process Using Artificial Neural Network (ANN),” Procedia Manufacturing Vol. 34, 2019, pp. 505 – 515.
[62] Jin, G., Li, W., and Gao, L., “An adaptive process planning approach of rapid prototyping and manufacturing,” Robotics andComputer-IntegratedManufacturing, Vol. 29, 2013, pp. 23 – 38.
[63] Yeung, H., Lane, B., Donmez, A., Fox, J. and Neira, J., Implementation of Advanced Laser Control Strategies for Powder Bed Fusion Systems, Procedia Manufacturing, College Station, TX, US, 2018. DOI: 10.1016/j.promfg.2018.07.112
[64] Lane B and Yeung, H. “Process Monitoring Dataset from the Additive Manufacturing Metrology Testbed (AMMT): Overhang Part X4,” J Research of NIST 125:125027, 2020, https://doi.org/10.6028/jres.125.027
[65] Lane, B., and Yeung, Ho, “Process Monitoring Dataset from the Additive Manufacturing Metrology Testbed (AMMT): “Three-Dimensional Scan Strategies”, Journal of Research of the National

Institute of Standards and Technology, Volume 124, Article No. 124033 (2019) https://doi.org/10.6028/jres.124.033

[66] Kim, F. , Garboczi, E. , Moylan, S. and Slotwinski, J. (2017), INVESTIGATION OF PORE STRUCTURE AND DEFECTS OF METAL ADDITIVE MANUFACTURING COMPONENTS USING X-RAY COMPUTED TOMOGRAPHY, 3rd International Conference on Tomography of Materials and Structures, Lund, SE, [online], https://doi.org/10.1016/j.addma.2017.06.011.

[67] Cook, P. and Murphy, A., "Simulation of melt pool behaviour during additive manufacturing: Underlying physics and progress," Additive Manufacturing, Vol. 31, 2020, #100909.

[68] Chen, H., Wei, Q., Zhang, Y. et al., "Powder-spreading mechanisms in powder-bed-based additive manufacturing: Experiments and computational modeling," Acta Materialia, Vol. 179, 2019, pp. 158 – 171.

[69] Xiang, Z., Yin, M., Deng, Z., Mei, X., and Yin, G., "Simulation of Forming Process of Powder Bed for Additive Manufacturing," J. Manuf. Sci. Eng., 138(8), 2016, 081002.

[70] Jia, T., Zhang, Y., and Chen, J. K., "Dynamic Simulation of Particle Packing With Different Size Distributions," J. Manuf. Sci. Eng., 133(2), 2011, 021011.

[71] Mohebbi, M. and Polshikhin, V., "Implementation of Nucleation in Cellular Automaton Simulation of Microstructural Evolution During Additive Manufacturing of Al Alloys," J. Additive Manufacturing, Vol. 36, 2020, #101726.

[72] Yang, Y., Gu, D., Dai, D., and Ma, C., "Laser energy absorption behavior of powder particles using ray tracing method during selective laser melting additive manufacturing of aluminum alloy," Materials & Design, vol. 143, 2018, pp. 12-19.

[73] Lane, B., Zhirnov, I., Mekhontsev, S., Grantham, S., Ricker, R., Rauniyar, S., and Chou, K., "Transient Laser Energy Absorption, Co-axial Melt Pool Monitoring, and Relationship to Melt Pool Morphology," Additive Manufacturing, vol. 36, 2020, article 101504.

[74] Reijonen, J., Revuelta, A., Riipinen, T., Ruusuvuori, K., and Puukko, P., "On the Effect of Shielding Gas Flow on Porosity and Melt Pool Geometry in Laser Powder Bed Fusion Additive Manufacturing," J. Additive Manufacturing, Vol. 32, 2020, #101030.

[75] Zhu, Q., Liu, Z. & Yan, J. "Machine Learning for metal additive manufacturing: Predicting temperature and melt pool fluid dynamics using physics-informed neural networks," Comput Mech 67, 619–635 (2021).

[76] Yang, Z, Lu, Y, Yeung, H, and Kirshnamurty, S. "3D Build Melt Pool Predictive Modeling for Powder Bed Fusion Additive Manufacturing," Proceedings of the ASME 2020 International Design Engineering Technical Conferences and Computers and Information in Engineering Conference. Volume 9: 40th Computers and Information in Engineering Conference (CIE). August 17–19, 2020. V009T09A046. ASME. https://doi.org/10.1115/DETC2020-22662.

[77] Patel, S. and Vlasea, M., "Melting modes in laser powder bed fusion," Materialia, vol. 9, 2020, article 100591.

[78] Panwisawas, C., Qiu, C., Anderson, M. et al., "Mesoscale Modelling of Selective Laser Melting: Thermal Fluid Dynamics and Microstructural Evolution," J. Computational Material Science, Vol. 126, 2017, pp. 479 – 490.

[79] Lu, L., Sridhar, N., Zhang, Y., "Phase Field Simulation of Powder Bed-Based Additive Manufacturing," Acta Materialia, Vol. 144, 2018 pp. 801 – 809.

[80] Akram, J., Chalavadi, P., Pal, D., and Stucker, B., “Understanding Grain Evolution in Additive Manufacturing Through Modeling,” J. Additive Manufacturing, Vol. 21, 2018, pp. 255 – 268.
[81] Rai, A., Helmer, H., and Korner, C., “Simulation of Grain Structure Evolution During Powder Bed Based Additive Manufacturing,” J. Additive Manufacturing, Vol. 13, 2017, pp. 124 – 134.
[82] Guraya, T., Singamneni, S., and Chen, Z., “Microstructure Formed During Selective Laser Melting of IN738LC in Keyhole Mode,” J. Alloys and Compounds, Vol. 792, 2019, pp. 151 – 160.
[83] Parry, L., Ashcroft, I., and Wildman, R., “Understanding the Effect of Laser Scan Strategy on Residual Stress in Selective Laser Melting Through Thermo-Mechanical Simulation,” J. Additive Manufacturing, Vol. 12, 2016, pp. 1 – 15.
[84] Gu, H., Gong, H., Pal, D., Rafi, K., Starr, T., and Stucker, B., “Influences of Energy Density on Porosity and Microstructure of Selective Laser Melted 17- 4PH Stainless Steel,” Proceedings of the Solid Freeform Fabrication Symposium, 2013.
[85] Qiu, C., Panwisawas, C., Ward, M., Basoalto, H., Brooks, J., Attallah, M., “On the role of melt flow into the surface structure and porosity development during selective laser melting,” Acta Materialia, Vol. 96, 2015, pp. 72 – 79.
[86] Brown, C. and Donmez, A., “Microstructure Analysis for Additive Manufacturing: A Review of Existing Standards,” Advanced Manufacturing Series (NIST AMS) - 100-3, 2016, doi: 10.6028/NIST.AMS.100-3.
[87] Feng, S., Lu, Y., and Jones, A., “Measured data alignments for monitoring metal additive manufacturing processes using laser powder bed fusion methods,” Proceedings of ASME 2020 International Design Engineering Technical Conferences and Computers and Information in Engineering Conference (IDETC/CIE 2020), Paper #: IDETC2020-22478.
[88] Feng, S., Lu, Y., and Jones, A., “Meta-data for in-situ monitoring of laser powder bed fusion processes,” Proceedings of ASME 2020 Manufacturing Science and Engineering Conference, 2020, Paper #: MSEC2020-8344.